Towards stabilization of the potential response of Mn(III) tetraphenylporphyrin-based solid-state electrodes with selectivity for salicylate ions

Tatiana A. Skripnikova[*a], Anna A. Starikova[b], Galina I. Shumilova[b] , Yuri E. Ermolenko[b], Andrey A. Pendin[b], Yulia G. Mourzina [*c]

[a]*St. Petersburg State University of Industrial Technologies and Design,*
191186, St. Petersburg, Bol'shaya Morskaya, 18, Russia
[b]*St. Petersburg State University*
198504, Russia, St. Petersburg, 7-9 Universitetskaya nab.
[c]*Peter Grünberg Institute PGI-8, Forschungszentrum Jülich GmbH, 52425 Jülich, Germany and JARA-FIT,*
52425 Jülich, Germany

Corresponding authors: t-star07@yandex.ru (Dr. T.A. Skripnikova)

telephone: 8-911-231-29-64,

y.mourzina@fz-juelich.de (Dr. Yu. Mourzina)

telephone: 49-2461-612364

Abstract We report a new type of solid-state electrode (type I) of a simple design with polyvinyl chloride membranes based on Mn(III) tetraphenylporphyrin and with graphite as the electronically conducting substrate. Enlargement of the membrane/graphite contact area by soaking graphite in the plasticizer with subsequent conditioning of the electrode at 30 °C allowed us to shorten the time required to achieve steady potential values of the sensors to just 3 days. These electrodes do not require a specially added RedOx system in the transducer layer. Stabilization of the EMF response of type I electrodes is compared to type II electrodes which contain a Cu^0/Cu^{2+} RedOx couple in the transducer layer. Type I sensors are suitable for measuring the salicylate ion concentration in the clinically important concentration range down to 2.5×10^{-4} M with a sensitivity to salicylate ion of -59.0 mV decade^{-1} in solutions with a high constant background of chloride ions of 0.12 M at pH=5.3, making this a promising technique for an effective design of solid-contact ion-selective electrodes with polymeric sensing membranes.

Keywords Solid-contact electrode, metalloporphyrin, graphite, large membrane/solid-contact area, oxygen-containing groups, salicylate ion

Introduction

Interest in studying the physicochemical properties of porphyrins and their metal complexes has arisen due to their essential role in many biological systems [1-4]. These substances have unique properties: their aromatic structure, the ability to acquire axial coordination and to form stable compounds with almost all metals from the periodic table. Owing to these properties, their field of application has been considerably extended over the last

few years. One such field is potentiometric sensing, i.e. the development of ion-selective electrodes (ISEs) with membranes containing complexes of porphyrins with various metals. ISEs are cost-efficient to produce, and they are simple to use and maintain, they allow the construction of portable instrumentation, non-destructive analysis and continuous *in-line* monitoring [5-8]. Because of these advantages, ISEs meet the requirements for various applications; in particular, they are frequently applied in pharmaceutical analysis [9].

Porphyrins and their derivatives are widely used as active compounds (ionophores) in ISE membranes [10-16]. The mechanism of action of these compounds is based not only on ion exchange, but also on the specific metal-ligand interaction in the presence of a charged metal center of metalloporphyrin, which makes it possible to use these compounds in the membranes of potentiometric sensors with improved selectivity for various anions [17,18].

We recently reported ISEs with membranes containing Mn(III) tetraphenylporphyrin – Mn(III)TPP$^+$, as a charged ionophore in various anionic forms of Mn(III)TPPX, with X$^-$=Cl$^-$, ClO$_4^-$, NO$_3^-$, SCN$^-$ [19]. The electrodes showed high selectivity for salicylate ion (Sal$^-$). However, these electrodes were of the conventional type with liquid contact, i.e. inner reference solution.

The salicylate anion and its derivatives are widely used as drugs with antimicrobial and analgesic action. Consumption of drugs based on salicylic acid is currently increasing. Therefore, it is becoming necessary to monitor salicylate ion concentrations in biological fluids. When a person takes such drugs, he should be aware that salicylate ions could already be present in the body, because acetylsalicylic acid is frequently used as an antiseptic and as a food preservative, and salicylate ions are found in fruit and vegetables and cosmetics. This is particularly relevant for people with thrombophlebitis, since acetylsalicylic acid is the main component in anticoagulant agents, and for people who take drugs that cannot be used together with salicylates (e.g. warfarin and tolbutamide).

One of the essential methods for detecting salicylate ions is based on the Trinder reaction, according to which the salicylate ion reacts with iron(III) ions to form colored complexes in acidic media. The disadvantage of this method is its low selectivity, because the colored complexes can be formed with many other compounds, such as endogenous phenol compounds, and some drugs, e.g., phenothiazine [20]. Electrochemical methods, cyclic voltammetry, amperometry, and potentiometry, matching the requirements of simple, low cost, miniaturizable, and portable methods have been applied for the determination of the salicylate anion. For example, salicylic acid, SA, was oxidized in alkaline solution at 0.7 V (vs SCE) and the product of oxidation was extracted on the electrode surface by solid-phase micro-extraction. The anodic peak current of the extracted species in differential pulse voltammograms was proportional to the concentration of salicylic acid in the range of 5.00 - 200 μM with a detection limit of 5.00 μM at alkaline pH [21]. The electro-oxidation of salicylic acid was enhanced at the multiwalled carbon nanotube (MWCNT) electrode compared to the glassy carbon electrode [22]. The sensor based on the MWCNT electrode demonstrated a linear range with SA concentration from 2.0×10^{-6} to 3.0×10^{-3} M and a low detection limit of 0.8×10^{-6} M at alkaline pH. The mechanism of electrochemical oxidation of SA on electrode surfaces at alkaline pH [22,23] and interaction of salicylate with the electrode materials [24] have been also investigated.

Several articles devoted to ion-selective potentiometric sensors for detecting salicylate ion have been published [6,25-32]. Unfortunately, a high concentration of ionophores in membranes, up to 3% w w^{-1}, often results in crystallization of the ionophore in the membrane phase or in high consumption of the ionophore [6,26,32]. Another drawback of membrane electrodes based on metalloporphyrins is associated with the short pH

range in which the electrodes have a theoretical potentiometric response [26,28]. Moreover, the presence of ionic additives in the composition of the membrane phase leads to a complicated structure of the electrode and to ambiguous interpretation of the ionophore's contribution to the electrode response [26,28,31,32]. Moreover, most known electrodes contain liquid contacts, which is disadvantageous in view of the miniaturization of ISEs and their maintenance [25,29-32]. Currently, neither of the proposed membrane formulations has optimum characteristics.

Various techniques are used for preparing solid-state electrodes with polymeric ion-selective membranes [33-41] and the state of the art was recently reviewed in [40]. Glassy carbon and graphite are widely used as solid-contact materials in solid-state ISEs [42-45]. It is well known that creating solid-contact electrodes with the conversion of charge carriers from ions to electrons at the membrane/contact interface encounters fundamental difficulties, which have not yet been completely solved [40,46,47]. In practice, one of the difficulties is insufficient stability of the electromotive force (EMF) response of the solid-contact electrodes with polymeric membranes [38,40]. In this report, we propose a new method for enlarging the contact area of the ISE-membrane/graphite solid contact interface by soaking graphite in a plasticizer with subsequent conditioning of the electrode at elevated temperature. This approach makes it possible to shorten the time required to achieve steady potential values to just 3 days for solid-contact electrodes with polyvinyl chloride (PVC) membranes containing metalloporphyrins and with graphite as the electronically conducting transducer. Based on this approach, a new type of solid-state electrode (type I) with a simple design was manufactured. These electrodes do not rely on the use of a specially added RedOx system in the transducer layer, while type II electrodes rely on the use of a RedOx system, which is common practice [48,46,49]. Stabilization of the potential response of type I electrodes was compared to that of type II electrodes containing a Cu^0/Cu^{2+} RedOx couple in the transducer layer.

Experimental methods

Chemicals and materials

MnTPPCl (Fig. 1), used as a charged ionophore in the ISE membranes, was synthesized as described in Ref.[19].

The purity of MnTPPCl was confirmed by thin layer chromatography (Silufol plates) and by spectrophotometry using the Shimadzu 1650UV spectrophotometer. Characteristic peaks at wavelengths of 378, 403, 479, 582 and 617 nm were registered in chloroform ($CHCl_3$).

Graphite rods EUZ-M were of the graphite grade whose mechanical properties show that most of the carbon was in the graphite grid. Graphite rods do not refer to the material which provides a mechanism with high capacity. Sodium salts with various anions X^-: Cl^-, Br^-, I^-, SCN^-, ClO_4^-, NO_3^-, NO_2^-, Sal^-, CH_3COO^-, SO_4^{2-}, HCO_3^-, $C_2O_4^{2-}$ (analytical grade) were obtained from NevaReaktiv, St. Petersburg, Russia. Aqueous solutions of these salts with different concentrations were prepared by sequential dilution using distilled water. Copper(II) sulfate and amino acids for the synthetic serum (Table S1) were supplied by Sigma-Aldrich Chemicals. Centrifugal filter devices Centricon-30 (molecular weight cut-off > 30,000) were from Millipore. Citrate-phosphate buffer was prepared as described in [50]. Cation exchange resin KU-23 was obtained from

NevaReaktiv, St. Petersburg. The organic solvents dibutyl phthalate (DBP), tetrahydrofuran (THF), and chloroform (CHCl$_3$) were obtained from Vekton, St. Petersburg, and were purified prior to use.
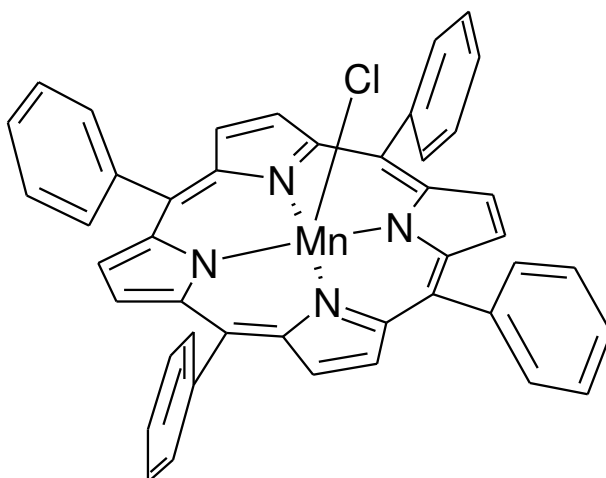

Fig. 1 Manganese tetraphenylporphyrin chloride (Mn(III)TPPCl)

Electrode preparation

To prepare type I electrodes, graphite rods with a diameter of 6 mm were soaked in DBP for 2-3 days to allow the DBP to penetrate into the graphite pores. The lateral surface of the rods was then insulated with PVC tubing, leaving only the butt ends open. To prepare type II electrodes, the butt ends of graphite rods (without treatment in DBP) were covered with a copper layer by the electrochemical deposition of copper from 0.3 M CuSO$_4$ by passing a cathodic current of 10 mA for 15-20 min.

It has been shown [51] that real graphite structures are porous and contain defects of different types. Water and oxygen are adsorbed on the graphite surface when the latter is in contact with aqueous electrolyte solutions. In the course of reducing molecular oxygen, carbon is charged positively, and is then able to attract anions [52,53]. Carbonyl, carboxyl, phenolic, hydroxyl and other oxygen-containing groups may be spontaneously formed on the graphite surface. Quantitative determination of these groups in graphite was performed [51]. Prolonged graphite soaking in solvent plasticizer, e.g. DBP, increases the area of the DBP/graphite interface. Penetration of DBP into graphite has been confirmed by IR spectroscopy [53,52].

The ISE membranes with two layers were prepared as follows: the outer (sensor) layer with pure ionic conductivity and the transducer layer with mixed ionic-electronic conductivity. The membrane cocktail for the sensor layers of electrode types I and II contained PVC, 33% (w w^{-1}), DBP, 66% (w w^{-1}), and Mn(III)TPPCl, 1% (w w^{-1}), corresponding to 0.02 M, dissolved in the cocktail solvent THF as described elsewhere [54,15,55]. An appropriate portion of the cocktail was poured into a Petri dish. After full evaporation of THF (~24 h), a membrane for the sensor layer was obtained with a thickness of about 0.5 mm. Discs with a diameter of 6 mm were cut from membranes of the sensor layer using a cork borer.

In order to prepare the transducer layer of the type I electrode, dispersed graphite was added to the membrane cocktail used for the sensor layer. The cocktail to dispersed graphite ratio was 2:1 by weight. In order to prepare a transducer layer of the type II electrode, the membrane cocktail used for the sensor layer was doped
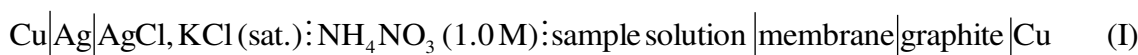
with dispersed graphite and cation exchanger resin KU-23 in a mixed Cu^{2+} + H^+ form. The cocktail cation exchanger resin KU-23 carbon black ratio was 2:1:0.6 by weight.

Cocktails of the transducer layers of type I and II electrodes were directly deposited on the top (butt ends) of the graphite rods of type I and II electrodes (prepared as described above in Section 2.2), respectively. Next, the membrane discs of the sensor layer were glued (the cocktail was used as glue) on top of the transducer layers. Four replicate ISEs of both types were used in the study.

Apparatus and measurements

Schematics of the proposed operation mechanisms of solid-state type I and II electrodes are shown in Fig. 2.

The potentiometric measurements with ISEs of both types were performed using an electrochemical cell with a double-junction Ag/AgCl reference electrode (Metrohm) containing saturated KCl as an inner reference solution and 1.0 M NH_4NO_3 in the outer chamber:
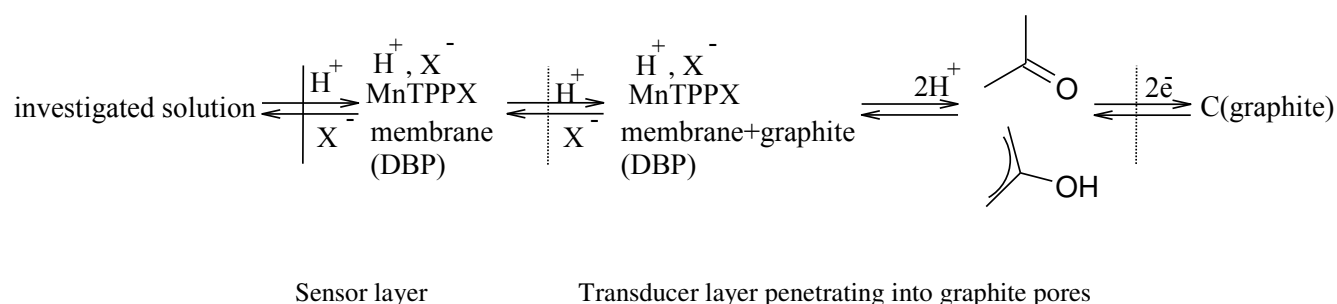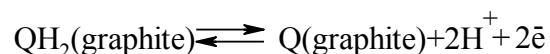
$$Cu \left| Ag \right| \underline{AgCl}, KCl\,(sat.) \vdots NH_4NO_3\,(1.0\,M) \vdots sample\,solution \left| membrane \right| graphite \left| Cu \right. \qquad (I)$$

A voltmeter/pH meter Mettler Toledo S40 with an input resistance of 10^{11} ohm was used for the EMF measurements. The pH measurements were performed using a pH meter pH-150 (Izmeritel, Gomel, Belarus) equipped with a glass pH electrode ESL-63-07 (Izmeritel, Gomel, Belarus) and the same reference electrode.
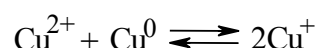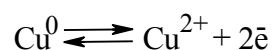
All measurements were performed at room temperature: 22±1 °C.

Scanning electron microscopy (SEM) investigations were performed at a Quanta 200 3D Fei Holland device.

Type I solid-state electrode:

$$QH_2(graphite) \rightleftharpoons Q(graphite) + 2H^+ + 2\bar{e}$$

Sensor layer   Transducer layer penetrating into graphite pores

Type II solid-state electrode:

$$Cu^0 \rightleftharpoons Cu^{2+} + 2\bar{e}$$

$$Cu^{2+} + Cu^0 \rightleftharpoons 2Cu^+$$

investigated solution $\rightleftarrows$ | $\begin{array}{c}H^+ \\ \\ X^-\end{array}$ | $\begin{array}{c}H^+, X^- \\ MnTPPX \\ membrane \\ (DBP)\end{array}$ $\rightleftarrows$ | $\begin{array}{c}H^+ \\ \\ X^-\end{array}$ | $\begin{array}{c}H^+, X^- \\ MnTPPX \\ membrane+graphite \\ +KU\text{-}23 \\ (DBP)\end{array}$ $\rightleftarrows$ $2H^+$ $\rightleftarrows$ ... $\begin{array}{c}2e^- \\ Cu^+ \\ \\ Cu^{2+}\end{array}$ C(graphite)

Sensor layer　　　　　Transducer layer penetrating into graphite pores
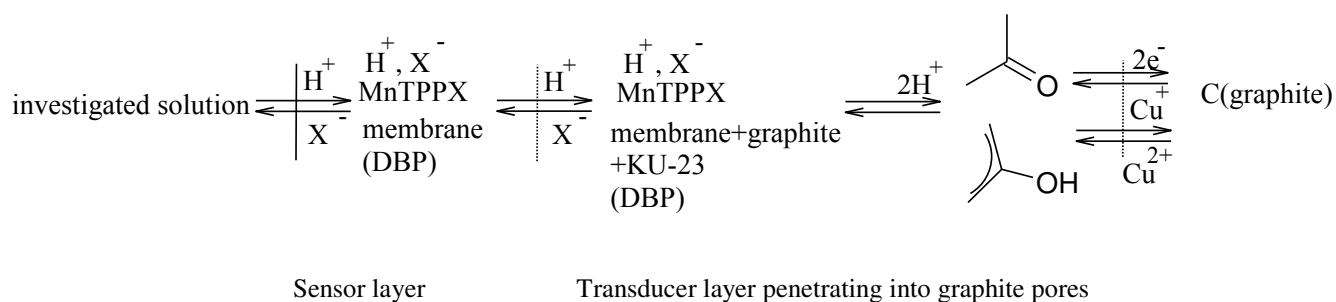
Fig. 2 Schematics of the operation mechanisms of type I and II solid-state electrodes. Symbol Q represents the oxygen-containing surface groups capable of oxidation and reduction

Results and discussion

Characterization of a graphite-dibutyl phthtalate interface

The state of a graphite-dibutyl phthtalate system was studied by IR-spectroscopy [52,53] to prove the DBP presence in graphite and determine the content of DBP in graphite. It was shown that DBP penetrated into graphite pores either upon the direct contact with DBP or upon the contact with the membrane plasticized with DBP. Electroactive compounds (ionophores) bought into contact with the DBP-plasticized membrane did no penetrate into the graphite structure. Analysis of characteristic frequencies in the spectra of the DBP-graphite system pointed to interactions between DBP and graphite unambiguously. As graphite in real conditions can have positive charges, it can be supposed that C^+ and DBP interact via donor-acceptor mechanism [52]. DBP and graphite can also interact via π-π-interactions mechanism [56,57]. This idea is confirmed by a recent study, where it is shown that the adsorption of dimethyl phthalate on carbon nanotubes is an endothermic spontaneous reaction and governed by the π-π electron interactions [57]. Adsorption of organic molecules on carbon materials as a complex interplay between electrostatic and non-electrostatic interaction was reviewed in [56]. Aromatic compounds are physisorbed on carbon materials essentially by dispersion interactions between the π-electrons of the aromatic ring and those of the graphene layers. Stronger interactions than the dispersion ones in these systems likely involve an electron donor-acceptor or charge-transfer mechanism [56]. The penetration of the plasticizer into the graphite pores makes the membrane solution interface bulky and extends the contact area between the electronic and ion conductor, which is favorable for the creation of the high-surface-area solid contacts [40].

　　　　Fig. 3 presents the SEM structural characterization of the graphite and graphite-dibutyl phthtalate system as used for the solid contact. One can observe more dense and ordered surface structure in the graphite-dibutyl phthtalate system compared to the initial graphite surface. The results of the SEM structural characterization are thus in agreement with the previous results of IR-spectroscopy pointing out to the penetration of DBP in graphite pores and interactions between DBP and graphite. This may be also one of the reasons for a better stability of the potential of the type I electrode as shown below.
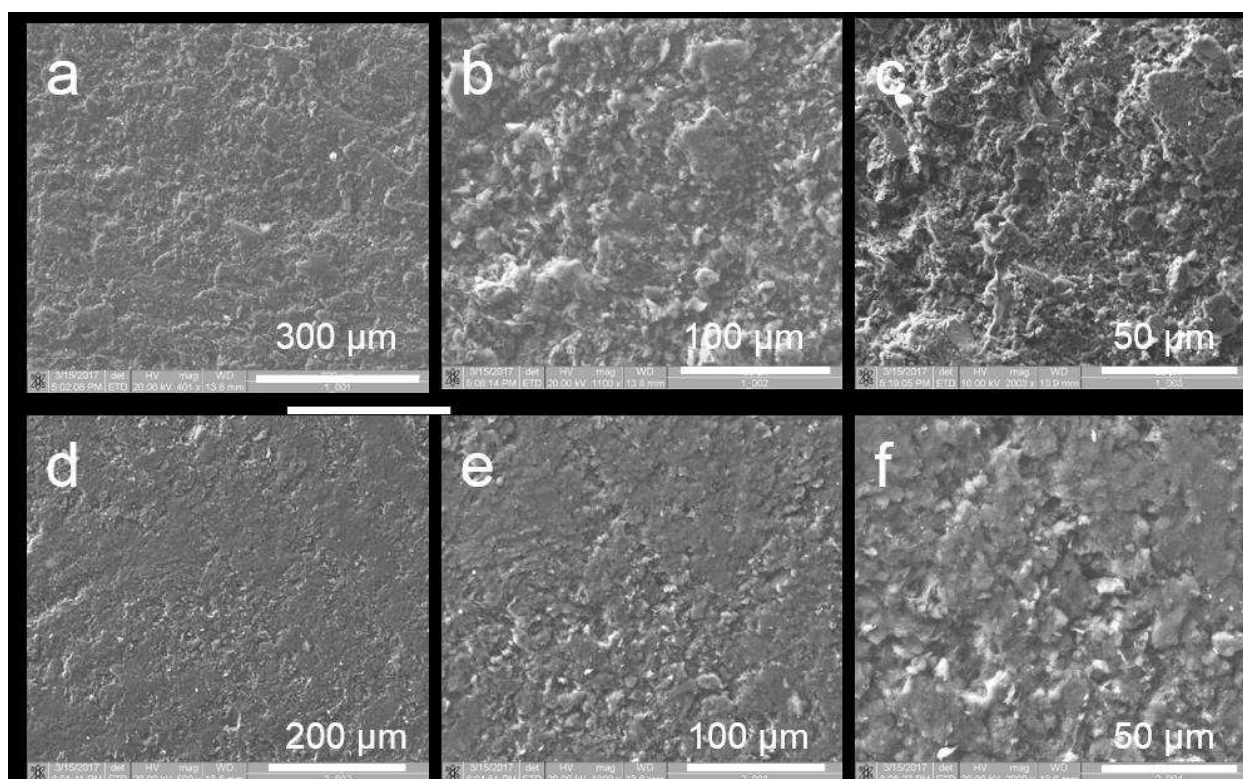
Fig. 3 SEM images of (a-c) graphite and (d-f) graphite-dibutyl phthtalate with different resolution used for the solid contact.

Influence of pH on the potentiometric response of solid-state electrodes

Among other anions, hydroxide forms the strongest complexes with metalloporphyrins. Hydroxide can influence the potentiometric response and the detection limits of ISEs with metalloporphyrin-based membranes, whatever the anion in the axial position of the metalloporphyrin complex. Therefore, it is necessary to study ISE behavior at different pH values.

The initial axial ligand in the metalloporphyrin complex is Cl^-. Therefore, pH interference was studied using NaCl as the background electrolyte. The aim was to achieve unambiguous interpretation of the pH influence on the potentiometric response of these solid-state electrodes, which is impossible in the case of salicylate ions. When the solution pH is lower than 5.0, salicylate precipitates as salicylic acid.

The potentials of the solid-state ISEs of types I and II in 0.1 M NaCl were measured over a wide range of pH from 2.3 to 10.2. The measurements started from pH 2 adjusted by additions of H_3PO_4. The pH was gradually increased up to pH 10.5 by the addition of small aliquots of aqueous NaOH. The ISEs reached stable potentials within 15 s at all pH values. The latter were controlled with a glass pH electrode. The pH dependences of the potentials of type I and II solid-state electrodes in 0.1 M NaCl are shown in Fig. 4.
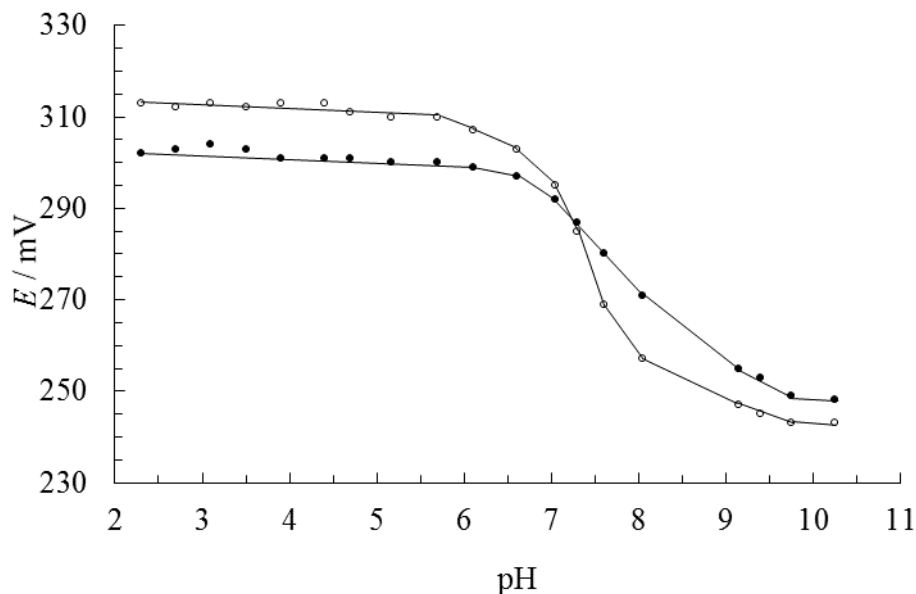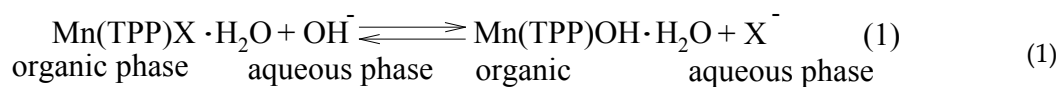
Fig. 4 pH dependence of the potentials of solid-state electrodes of type I (○) and II (●) in 0.1 M NaCl

It can be seen that the dependence of the ISE potentials on pH exhibits a sigmoid curve with two plateaus at pH<6.5 and at pH>9.5. Similar results were also displayed by conventional ISEs with the same membrane [19].

Within the pH range from 2.0 to 6.5, OH⁻ ion activity is too low, and OH⁻ cannot compete with Cl⁻ ion for the axial coordination position in the metalloporphyrine molecule. However, at pH>6.5, hydroxide is able to replace chloride according to the reaction below:

$$Mn(TPP)X \cdot H_2O + OH^- \rightleftharpoons Mn(TPP)OH \cdot H_2O + X^- \qquad (1)$$
organic phase aqueous phase organic aqueous phase

This reaction was confirmed by a two-phase spectrophotometric titration of the Mn(III)TPPCl with potentiometric pH control [58].

Slope, selectivity and response time of the solid-state electrodes

The dynamic range and slope of the electrode function in solutions of NaX sodium salts with different anions (X⁻ = Cl⁻, Sal⁻, SCN⁻, ClO₄⁻, Br⁻, I⁻, CH₃COO⁻, NO₃⁻, NO₂⁻) was determined by EMF measurements. Prior to the measurements, the ISEs were conditioned in 0.1 M NaX solutions for 2-3 days to ensure full conversion of Mn(III)TPPCl in the membrane into the respective Mn(III)TPPX form. The measurements were performed at pH 5.3 maintained with citrate-phosphate buffer. This buffer was chosen because preliminary studies showed negligible interference from citrate and hydrogen phosphate ions on the potentials of electrodes based on Mn(III)TPPCl.

The values of the slopes, lower detection limits, and linear ranges of the electrodes under investigation are presented in Table 1.

8

Table 1 Values of slopes (*S*), lower detection limits (*DL*), and linear ranges (*LR*) of type I and II electrodes of in various NaX solutions at pH 5.3

NaX	S / mV $\log(a_X)^{-1}$		DL / M		LR / M	
	type I	type II	type I	type II	type I	type II
NaSCN	−59.7	−59.1	1.0×10^{-5}	1.0×10^{-5}	1.0×10^{-4} - 5.0×10^{-4}	1.0×10^{-4} - 5.0×10^{-4}
NaSal	−59.0	−58.4	1.0×10^{-5}	1.0×10^{-5}	1.0×10^{-4} - 5.0×10^{-4}	1.0×10^{-4} - 5.0×10^{-4}
NaClO$_4$	−52.0	−51.5	1.0×10^{-4}	1.0×10^{-4}	1.0×10^{-4} - 5.0×10^{-4}	1.0×10^{-4} - 5.0×10^{-4}
NaBr	−47.0	−44.0	5.0×10^{-4}	5.0×10^{-4}	1.0×10^{-4} - 5.0×10^{-4}	1.0×10^{-3} - 1.0×10^{-3}
NaNO$_2$	−42.7	−43.1	1.0×10^{-3}	1.0×10^{-3}	1.0×10^{-3} - 5.0×10^{-3}	1.0×10^{-3} - 5.0×10^{-3}
NaCl	−36.5	−36.5	5.0×10^{-4}	5.0×10^{-4}	1.0×10^{-3} - 5.0×10^{-3}	0.1×10^{-3} - 5.0×10^{-3}
NaNO$_3$	−36.0	−35.6	5.0×10^{-4}	5.0×10^{-4}	0.1×10^{-3} - 5.0×10^{-3}	1.0×10^{-3} - 5.0×10^{-3}

Both types of electrodes exhibit Nernstian responses in NaSal and NaSCN solutions. Clinically relevant concentrations of salicylate are in the millimolar range.

The potentiometric selectivity of the electrodes assuming salicylate to be the primary ion was determined by the separate solutions method using 0.1 M sodium salts of salicylate and X$^-$ as a respective interfering anion. The selectivity coefficients were calculated as:

$$\log K_{Sal/X} = -\frac{E_X - E_{Sal}}{S}, \tag{2}$$

where E_{Sal}, E_X are the EMF values measured in NaSal and in NaX solutions, respectively, and *S* is the slope of the electrode function. The selectivity coefficients of the electrodes under investigation, together with that of the conventional ISEs with liquid contact (inner filling solution) in aqueous solutions, are presented in Table 2.

**Table 2** Selectivity coefficients of the electrodes with membranes based on Mn(III)TPPCl

Anion X$^-$	$\log K_{Sal/X}$		
	Conventional ISE[19]	Type I	Type II
Sal$^-$	0.00	0.00	0.00
NO$_3^-$	−2.78	−2.74	−2.67
NO$_2^-$	−2.16	−2.13	−2.11
SCN$^-$	0.32	0.24	0.30
Cl$^-$	−2.43	−2.64	−2.60

Br$^-$	−2.30	−2.45	−2.42
I$^-$	−1.65	−1.63	−1.51
ClO$_4^-$	−1.01	−1.19	−1.01
CH$_3$COO$^-$	−1.81	−2.04	−1.96
SO$_4^{2-}$	-3.64	-4.01	-3.91
HCO$_3^-$	-2.36	-2.39	-2.37
C$_2$O$_4^{2-}$	-2.42	-2.36	-2.30

The electrodes (type I and type II) show the following selectivity series for anions:

SCN$^-$ > Sal$^-$ > ClO$_4^-$ > I$^-$ > CH$_3$COO$^-$ > NO$_2^-$ > C$_2$O$_4^{2-}$ > HCO$_3^-$ > Br$^-$ > Cl$^-$ > NO$_3^-$ > SO$_4^{2-}$,
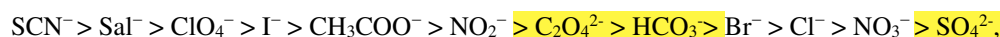
which differs from the selectivity series (Hofmeister series) for the electrodes based on quaternary ammonium bases [59,60]:

ClO$_4^-$ > IO$_4^-$ > SCN$^-$ > Sal$^-$ > I$^-$ > Br$^-$ > NO$_2^-$ > Cl$^-$ > HCO$_3^-$ > F$^-$
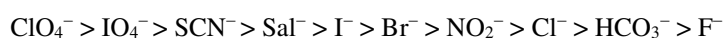
The selectivities of the lipophilic PVC plasticized membranes based on anion-exchangers are determined by variation of the free energy of solvation during migration of ions being determined from aqueous solutions to the membrane phase resulting in the Hofmeister series for anions whereby more lipophilic anion such as ClO$_4^-$ is preferentially incorporated into the membrane phase [59,61,62]. To create electrodes selective to Sal$^-$ changing the Hofmeister series should be employed. Deviation from the Hofmeister series can be achieved due to the specific interactions of ions in the solution with the active components introduced into the membrane phase. Incorporation of metalloporphyrins as an active component into the membrane phase can result in the selectivity of the membrane sensors to a particular sort of ions due to the specific interaction of the active component with the ions in the solution [2,7]. Electrode selectivity of these membranes in not governed by anion lipophilicity as in the case of anion-exchangers. The membranes with Mn(III)TPP as an active component deviate from the Hofmeister series due to the selectivity imparted by the interaction of anion as an axial ligand with the manganese centre of the porphyrin macrocycle [61]. The relative affinity of an anion as an axial ligand dictates selectivity. For example, perchlorate is considered to be a weak Mn(III) porphyrin axial ligand and this may account for a low potentometric response to this lipophilic anion [59,63]. The SO$_4^{2-}$, PO$_4^{3-}$, and NO$_3^-$ do not yield a product with the Mn(III) porphyrin complex [64,65], which explains a low potentiometric response to these anions. The easy of precipitation of Mn(III) porphyrins complex was found to follow the order I$^-$ > Br$^-$ > Cl$^-$ > F$^-$ [65] and is in agreement with selectivity determined for the sensor. It was additionally supposed that π-π interactions with porphyrin ring might be responsible for the initial extraction of salicylate into the ISE membrane [60].

ISEs with membranes based on Mn(III)TPPCl, whether with solid contact or with aqueous inner reference solution, showed selectivity for salicylate and thiocyanate anions over a number of interferences, including perchlorate, Table 2. These data are consistent with our earlier findings [19]. As seen, the selectivity series for the electrode with an inner reference solution correspond to the selectivity series for the solid-state electrodes, Table 2. This confirms that our preparation methods for solid-state electrodes were successful.

The response time of type I electrodes is 10 s at concentrations of 10^{-5} to 10^{-2} M, and 5-10 s at 0.1-1.0 M. Type II electrodes showed a slower response: 20-30 s over the whole dynamic range. The variation of the potential value of type I electrodes is 5-7 mV at concentrations 10^{-5} to 10^{-3} M and 1-2 mV at concentrations 10^{-2}

to 1.0 M. The variation of the potential value of type II electrodes is 10-15 mV. Type I solid-state electrodes exhibit faster and more reversible potentiometric response than type II electrodes.

A series of type I electrodes have been prepared and used only in the diluted solutions of salicylate ions in a concentration range of 10^{-7} - 10^{-4} M. When the electrodes were used only in diluted solutions, the electrode demonstrated a linear response with a slope of 58.8 mV dec^{-1} down to 2×10^{-6} M of salicylate ions with a detection limit of 1×10^{-6} M. The response time of type I electrodes in this concentration range was 10-15 s. The variation of the potential value was 7-8 mV. If the electrodes were used in the higher concentration ranges of Sal$^-$ ions, the sensitivity in a lower concentration range was diminished seriously and required a prolonged (up to 24 h) washing procedure in a 10^{-7} M Sal to regenerate the electrode for working in the lower concentration ranges.

A test for the presence of a water layer [47] was also carried out. For this purpose, the investigated electrodes were kept in a solution of 0.1 M NaSal for 30 min, and after that the electrodes were placed in a solution of 0.1 M NaCl. The potentials of the solid-state electrodes changed rapidly and remained stable during all the measurements. Then the electrodes were placed again in NaSal solution. The potentials of both types of investigated electrodes of returned to their initial value. This confirms that ISEs do not have an aqueous layer between the solid contact and the sensing membrane.

The selectivity for salicylate ions makes the type I electrode a promising candidate for salicylate ion control in medical and biological applications. Therefore, the sensor response was studied by measuring the ISE potentials in model solutions with a high constant background concentration of 0.12 M NaCl and different concentrations of NaSal at pH 5.3. This concentration of Cl$^-$ ions was chosen because it corresponds to the average total concentration of chloride ions in urine of 110 to 250 mmol day^{-1}, while the daily amount of urine is 1.2-1.5 liters. Other organic ions are found in smaller amounts in urine and will not interfere with the determination of Sal$^-$, as shown previously in [6]. pH 5.3 is typical of urine [66]. The sensor response of type I solid-state electrodes in the model solutions is shown in Fig. 5.
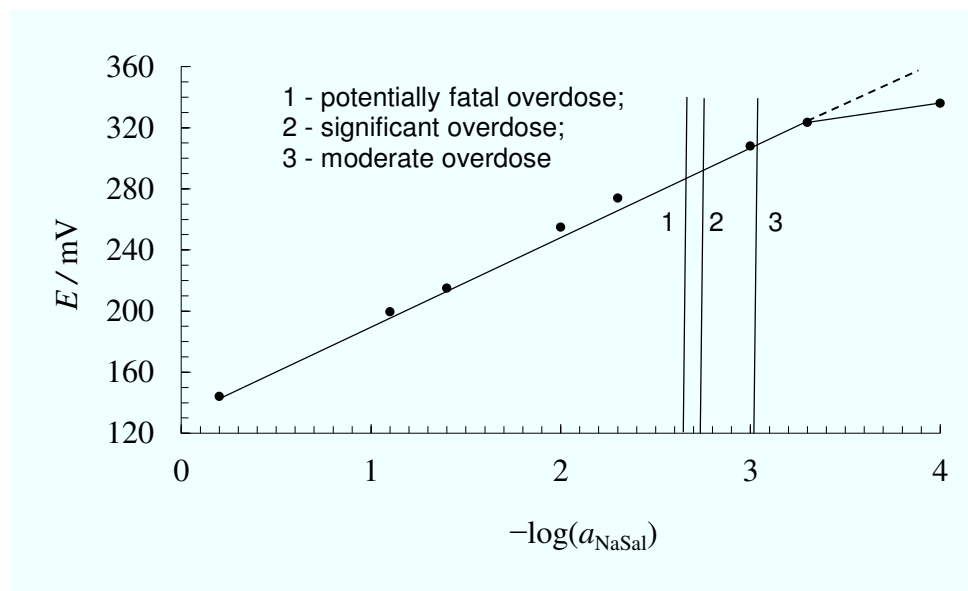

Fig. 5 Potentials of type I solid-state electrodes in NaSal +NaCl (0.12 M) solutions at pH 5.3

As can be seen, the concentration of salicylate ion may be determined down to 2.5×10^{-4} M with a constant background of 0.12 M chloride ions. Three clinical salicylate ion concentrations are shown in Figure 5,

which correspond to varying degrees of salicylate overdose: potentially fatal overdose (2.2 mmol l^{-1}), significant overdose (1.7 mmol l^{-1}) and moderate overdose (0.9 mmol l^{-1}). The electrodes retain Nernstian slopes −58.14 mV log(a_{Sal})$^{-1}$ in the clinically important concentration range of salicylate. Therefore, these electrodes may provide an alternative device for the determination of salicylate in urine in a wide range of clinical concentrations of salicylate ions.

The reproducibility of the slope of the calibration curves was within ±1.2 mV decade^{-1} over a period of 2 months.

To illustrate the feasibility of the electrode in practical analysis, it was employed to determine "free" salicylate in synthetic and human blood serum samples using a spike procedure [67]. The clinical range of salicylate in serum required for anti-inflammatory therapy is 15 - 30 mg dl^{-1} (1.1 - 2.2 mM) [68]. Signs and symptoms of toxicity begin to appear at levels higher than 30 mg/dL. A 6-hour salicylate level higher than 100 mg/dL is considered potentially lethal and is an indication for hemodialysis. Recovery studies were conducted with a synthetic serum samples containing 0.9×10^{-3} - 6.2×10^{-3} M salicylate. The composition of the synthetic serum sample is given in Table S1 [69,70]. A synthetic serum sample solution was diluted (1:3) with a 0.05 M phosphate buffer, pH 5.8. The calibration curve was prepared using salicylate standards prepared in 88.8 mM NaCl and diluted (1:3) with a 0.05 M phosphate buffer, pH 5.8. Human blood serum samples were ultrafiltrated through centrifugal filter devices Centricon-30 (molecular weight cut-off > 30,000). The samples were diluted (1:2) with a 0.05 M phosphate buffer, pH 5.8. The recovery results in Table 3 demonstrate that the type I electrodes can be used for the selective monitoring of salicylate level in biological samples in the clinically important concentration range.

Table 3. Recovery of salicylate in synthetic and blood serum samples using a type I Sal^{-} -selective electrode.

Salicylate content in a diluted human blood serum sample, mM [a]	Salicylate added, mM	Salicylate found, mM	Recovery, %, [b]
synthetic serum samples			
	0.92	0.96	104.3
	1.0	1.02	102.0
	1.80	1.86	103.3
	3.80	3.75	98.7
	6.20	6.27	101.1
human blood serum			
0.62	0	0.81	131
0.62	0.25	0.94	108
0.62	0.50	1.11	99

[a] - determined by the colorimetry method in a local hospital; [b] - three replicates were performed.

Comparison of the performance of salicylate solid-state sensors

It should be noted that salicylate-selective solid-state electrodes based on Mn(III)TPPCl have never been comprehensively studied. Table 4 compares the membrane compositions, slopes of the electrode functions, linear

12

ranges, detection limits, working pH ranges, and response times of the salicylate-selective solid-state electrodes reported previously [27,28,70,71].

Table 4 Comparison of different parameters of the salicylate-selective solid-state electrodes based on Mn(III)TPPCl (type I) with other previously reported salicylate solid-state sensors

Parameters / Ref.		This work	[27]	[27]	[28]	[70]	[71]
Membr. comp. ($\%\ w\ w^{-1}$)	PVC	33.0	32.0	38.5	25.0	30.0	32.0
	plasticizer	66.0 DBP	65.8 DOP	57.6 DOP	50.0 NPOE	63 NPOE	63 NPOE
	MAC	1.0 MnTPPCl	2.2 Al salophen	2.8 Sn salophen	20.0 CuTPP-GO	5.0 TCN	5.0 TOA BSB
	Add.	-	-	1.1 TOMACl	5.0 NaTPB	2.0 HTAB	20 PctAlCl
Slope (mV dec^{-1})		−59.0	−59.2	−57.2	−57.8	−59.2	−57.9
Linear range (M)		5.0×10^{-5} - 1.0 [a]	1×10^{-6} - 1×10^{-1}	1×10^{-6} - 1×10^{-1}	5×10^{-7} - 5×10^{-1}	1×10^{-6} - 1×10^{-2}	1×10^{-4} - 1×10^{-1}
Detection limit (M)		1.0×10^{-5} [a]	1×10^{-6}	8×10^{-7}	8×10^{-8}	7×10^{-7}	-
Response time		~10 s	~20-30 s	~20-30 s	~10-20 s	<10 s	~10 s

* - a detection limit of 1×10^{-6} M can be achieved when working in a concentration range of 10^{-7} - 10^{-4} M.

The proposed sensor (type I) is superior to previously reported salicylate-selective solid-state sensors in terms of membrane composition and response time. It is more cost-effective, since it requires a lower consumption of ionophore, while demonstrating a Nernstian response. Moreover, this electrode does not require the introduction of ionic additives. The sensor is applicable in the clinically important concentration range of salicylate. The sensor performance demonstrates that stabilization of the electrode potential may be effectively achieved using the proposed technique.

Stability of the potentiometric response of the solid-state electrodes over time

The interpretation of the directly measured signal, the EMF, in terms of the activity or the concentration of the analyte in the sample relies on the ISE calibration parameters. Therefore, the stability of these parameters, i.e. the slope of the electrode function, S, and the standard potential value, $E^{\ominus}$, are of great importance for the practical use of ISEs. The slope of the calibration curve is typically stable over time. However, the standard potential tends to vary with time, especially for solid-state ISEs [40,47,48].

The long-term stability of the ISE potentials was studied by measuring the EMF in 0.1 M NaSal as a reference solution over a period of about two months. The EMF values registered for type I and II electrodes of in this solution at 22 °C are shown in Fig. 6.
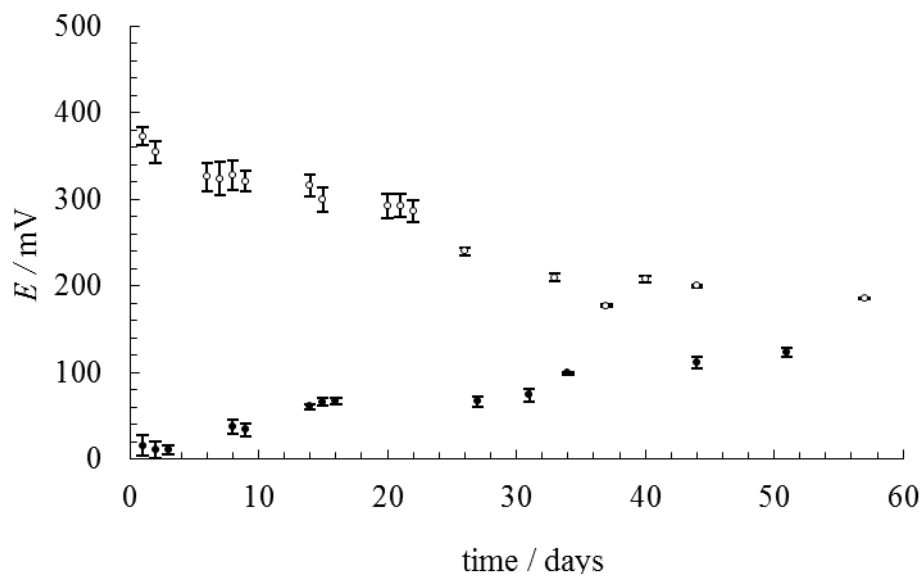
Fig. 6 Potentials of electrodes of types I (○) and II (●) in 0.1 M NaSal at 22 °C over time

Immediately after immersing ISEs into 0.1 NaSal, the EMF was measured every 30 minutes for the first 4 hours. During this initial time, the difference between the values of the electrode potentials within a set of 4 replicate type I electrodes was 5 to 7 mV. Later, the measurements were performed at intervals of several days. After 20 days of contact with the solution, type I electrodes showed a variation in the potential value of 3-5 mV within a set of electrodes. Type II electrodes displayed a more significant variation of the potential values of 15 to 20 mV. The potential of the type I electrodes achieved a steady value of 200 to 210 mV after 33 days of measurements. At days 40 and 60, the type I electrodes showed the same value. No significant electrode potential deviations from the steady value were observed. It can be assumed that the decrease in the potential values of type I electrodes could be caused by a reduction of carbonyl groups on the graphite surface to hydroxyl groups. The potential of type II electrodes achieved a steady value of 200 to 210 mV similar to type I electrodes. However, type II electrodes did not demonstrate a steady value even at day 50. We assume that an increase of the standard electrode potential for type II electrodes in the first days of the experiment corresponds to the oxidation of copper. Copper ions appear in the transducer layer because atmospheric oxygen absorbed by the membrane oxidizes the metal copper deposited on the graphite surface. The positive charge of copper ions is counterbalanced by salicylate ions. Apparently, the RedOx equilibria, where phenolic groups and copper are involved, facilitate the transition from electronic to ionic conductivity in the transducer layer and stabilize the ISE potentials.

Unlike type II electrodes with a copper layer deposited on the graphite substrate, type I electrodes do not contain any specially added RedOx agents. Therefore, the RedOx buffer capacity of type I electrodes is lower. This appears to be the reason for the faster change of the potentials in these electrodes over time.

The RedOx reaction rate can be increased by conditioning the electrodes at elevated temperatures. Therefore, the ISEs immersed in 0.1 M NaSal were conditioned at 30 °C and 50 °C in a thermostat for 3 days. After that, the EMF values were measured in 0.1 M NaSal at room temperature (22 °C). The dynamics of the electrode potentials after conditioning in 0.1 M NaSal over time are shown in Fig. 7.
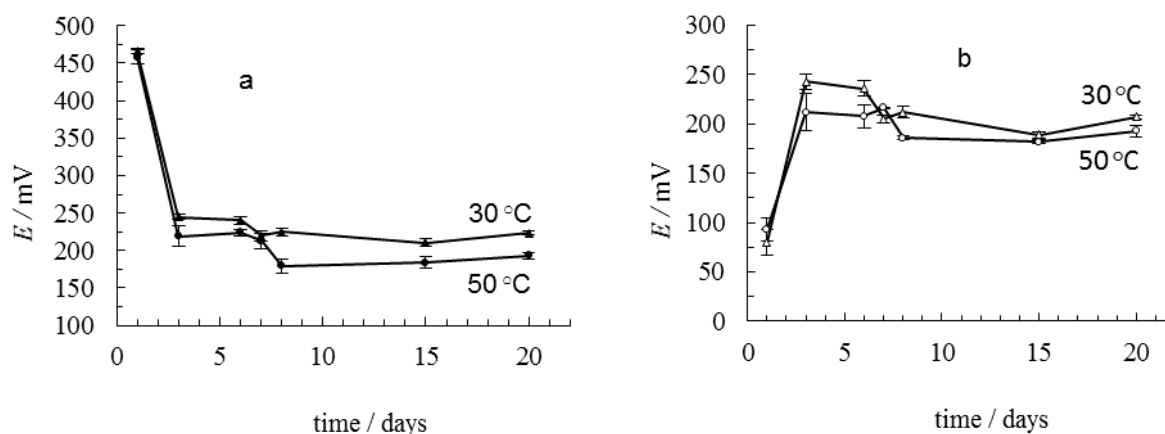
14

Fig. 7 Potentials of the electrodes in 0.1 M NaSal over time. Type I (a): conditioning at t=30 °C (▲) and t=50 °C (●), type II (b) conditioning at: t=30 °C (Δ), t=50 °C (○)

As can be seen in Fig. 7, both types of electrodes achieve potential values of about 210 mV after 3 days, which is significantly faster than without conditioning at elevated temperature. Therefore, conditioning of the electrodes in the solution at 30 °C may be recommended to speed up stabilization of the ISE potentials in a reference solution at a steady value.

Conclusions

We propose a new type of solid-state salicylate-selective electrode based on Mn(III)TPPCl with a simple design and discuss the dynamic processes, which occur in the described systems of the solid contacts. The proposed solid contact allows a faster and more reversible potentiometric response to be achieved. This effective method of manufacturing solid-contact electrodes without specially added RedOx agents in the transducer layer (type I electrodes) and conditioning at 30 °C may be recommended for wider application, in particular for ISEs with membranes based on porphyrins and metalloporphyrins. The solid-contact electrodes of this type with membranes based on manganese tetraphenylporphyrins were applied for measuring salicylate ions in biological samples.

Acknowledgements

References

1. Gao W-Y, Chrzanowski M, Ma S (2014) Metal-metalloporphyrin frameworks: a resurging class of functional materials. Chemical Society Reviews 43 (16):5841-5866. doi:10.1039/C4CS00001C

2. Biesaga M, Pyrzyńska K, Trojanowicz M (2000) Porphyrins in analytical chemistry. A review. Talanta 51 (2):209-224. doi:http://dx.doi.org/10.1016/S0039-9140(99)00291-X

3. Koposova E, Liu X, Pendin A, Thiele B, Shumilova G, Ermolenko Y, Offenhausser A, Mourzina Y (2016) Influence of Meso-Substitution of the Porphyrin Ring on Enhanced Hydrogen Evolution in a Photochemical System. Journal of Physical Chemistry C 120 (26):13873-13890. doi:10.1021/acs.jpcc.6b01467

4. Koposova E, Shumilova G, Ermolenko Y, Kisner A, Offenhausser A, Mourzina Y (2015) Direct electrochemistry of cyt c and hydrogen peroxide biosensing on oleylamine- and citrate-stabilized gold nanostructures. Sensors and Actuators B-Chemical 207:1045-1052. doi:10.1016/j.snb.2014.07.105

5. Kimmel DW, LeBlanc G, Meschievitz ME, Cliffel DE (2012) Electrochemical Sensors and Biosensors. Analytical Chemistry 84 (2):685-707. doi:10.1021/ac202878q

6. Zhang X-B, Guo C-C, Jian L-X, SHEN G-L, Yu R-Q (2000) Bismetalloporphyrin Complexes as Ionic Carriers for a Salicylate-Sensitive Electrode. Analytical sciences 16 (12):1285-1289

7. Paolesse R, Nardis S, Monti D, Stefanelli M, Di Natale C (2017) Porphyrinoids for Chemical Sensor Applications. Chemical Reviews 117 (4):2517-2583. doi:10.1021/acs.chemrev.6b00361

8. Ermolenko Y, Yoshinobu T, Mourzina Y, Levichev S, Furuichi K, Vlasov Y, Schoning MJ, Iwasaki H (2002) Photocurable membranes for ion-selective light-addressable potentiometric sensor. Sensors and Actuators B-Chemical 85 (1-2):79-85. doi:10.1016/s0925-4005(02)00056-4

9. Santos EMG, Araújo AN, Couto CMCM, Montenegro MCBSM, Kejzlarová A, Solich P (2004) Ion selective electrodes for penicillin-G based on Mn(III)TPP-Cl and their application in pharmaceutical formulations control by sequential injection analysis. Journal of Pharmaceutical and Biomedical Analysis 36 (4):701-709. doi:http://dx.doi.org/10.1016/j.jpba.2004.08.006

10. Bühlmann P, Pretsch E, Bakker E (1998) Carrier-Based Ion-Selective Electrodes and Bulk Optodes. 2. Ionophores for Potentiometric and Optical Sensors. Chemical Reviews 98 (4):1593-1688. doi:10.1021/cr970113+

11. Chen LD, Zou XU, Bühlmann P (2012) Cyanide-Selective Electrode Based on Zn(II) Tetraphenylporphyrin as Ionophore. Analytical Chemistry 84 (21):9192-9198. doi:10.1021/ac301910c

12. Johnson RD, Bachas LG (2003) Ionophore-based ion-selective potentiometric and optical sensors. Analytical and Bioanalytical Chemistry 376 (3):328-341. doi:10.1007/s00216-003-1931-0

13. Lvova L, Di Natale C, Paolesse R (2013) Porphyrin-based chemical sensors and multisensor arrays operating in the liquid phase. Sensors and Actuators B: Chemical 179:21-31. doi:http://dx.doi.org/10.1016/j.snb.2012.10.014

14. Shahrokhian S (2001) Lead Phthalocyanine as a Selective Carrier for Preparation of a Cysteine-Selective Electrode. Analytical Chemistry 73 (24):5972-5978. doi:10.1021/ac010541m

15. Shirmardi-Dezaki A, Shamsipur M, Akhond M, Sharghi H (2013) Cyanide selective electrodes based on a porphyrinatoiron(III) chloride derivative. Journal of Electroanalytical Chemistry 689:63-68. doi:http://dx.doi.org/10.1016/j.jelechem.2012.10.029

16. Vlascici D PI, Chiriac VA, Fagadar-Cosma G, Popovici H, Fagadar-Cosma E (2013). Chemistry Central Journal 7:1-7

17. Farhadi K, Maleki R, Hosseinzadeh Yamchi R, Sharghi H, Shamsipur M (2004) [Tetrakis (4-N, N-dimethylaminobenzene) porphyrinato]-manganese (III) acetate as a novel carrier for a selective iodide PVC membrane electrode. Analytical sciences 20 (5):805-809

18. Santos EMG, Araújo AN, Couto CMCM, Montenegro MCBSM (2006) Construction and evaluation of PVC and sol–gel sensor membranes based on Mn(III)TPP-Cl. Application to valproate determination in pharmaceutical preparations. Analytical and Bioanalytical Chemistry 384 (4):867-875. doi:10.1007/s00216-005-0170-y

19. Starikova TA, Shumilova GI, Valiotti AB (2013) Electrochemical charactreistics of membranes based on Mn(III) tetraphenylporphyrin. In English. Russian Journal of Electrochemistry 49 (9):856-862. doi:10.1134/S1023193513090115

20. Trinder P (1954) Rapid determination of salicylate in biological fluids. Biochemical Journal 57 (2):301-303

21. Zhu Y, Guan X, Ji H (2009) Electrochemical solid phase micro-extraction and determination of salicylic acid from blood samples by cyclic voltammetry and differential pulse voltammetry. Journal of Solid State Electrochemistry 13 (9):1417-1423. doi:10.1007/s10008-008-0707-z

22. Zhang W-D, Xu B, Hong Y-X, Yu Y-X, Ye J-S, Zhang J-Q (2010) Electrochemical oxidation of salicylic acid at well-aligned multiwalled carbon nanotube electrode and its detection. Journal of Solid State Electrochemistry 14 (9):1713-1718. doi:10.1007/s10008-010-1014-z

23. do Prado TM, Machado SAS (2016) Spectroelectrochemical study of salicylate in alkaline medium. Journal of Solid State Electrochemistry 20 (9):2569-2574. doi:10.1007/s10008-015-3106-2

24. Batista EA, Temperini MLA (2007) An in situ SERS and FTIRAS study of salicylate interaction with copper electrode. Journal of Solid State Electrochemistry 11 (11):1559-1565. doi:10.1007/s10008-007-0357-6

25. Shishkanova TV, Videnská K, Antonova SG, Kronďák M, Fitl P, Kopecký D, Vrňata M, Král V (2014) Application of polyaniline for potentiometric recognition of salicylate and its analogues. Electrochimica Acta 115:553-558. doi:http://dx.doi.org/10.1016/j.electacta.2013.10.214

26. Shahrokhian S, Hamzehloei A, Bagherzadeh M (2002) Chromium(III) Porphyrin as a Selective Ionophore in a Salicylate-Selective Membrane Electrode. Analytical Chemistry 74 (14):3312-3320. doi:10.1021/ac020099n

27. Shahrokhian S, Amini MK, Kia R, Tangestaninejad S (2000) Salicylate-Selective Electrodes Based on Al(III) and Sn(IV) Salophens. Analytical Chemistry 72 (5):956-962. doi:10.1021/ac990749w

28. Poursaberi T, Hassanisadi M (2012) Application of metalloporphyrin grafted-graphene oxide for the construction of a novel salicylate-selective electrode. Journal of Porphyrins and Phthalocyanines 16 (10):1140-1147. doi:10.1142/S1088424612501143

29. Messick MS, Krishnan SK, Hulvey MK, Steinle ED (2005) Development of anion selective polymer membrane electrodes based on lutetium(III) porphyrins. Analytica Chimica Acta 539 (1–2):223-228. doi:http://dx.doi.org/10.1016/j.aca.2005.03.049

30. Malinowska E, Niedziółka J, Roźniecka E, Meyerhoff ME (2001) Salicylate-selective membrane electrodes based on Sn(IV)- porphyrins: differences in response mechanism and analytical performance. Journal of Electroanalytical Chemistry 514 (1–2):109-117. doi:http://dx.doi.org/10.1016/S0022-0728(01)00615-5

31. Luo E-P, Chai Y-Q, Yuan R, Dai J-Y, Xu L (2009) Highly salicylate-selective membrane electrode based on a new thiomacrocyclic Schiff base complex of binuclear copper(II) as neutral carrier. Desalination 249 (2):615-620. doi:http://dx.doi.org/10.1016/j.desal.2008.12.054

32. Ganjali MR, Norouzi P, Faridbod F, Rezapour M, Ahmadi A (2007) Application of Tetra Cyclohexyl Tin(IV) as an Anionic Carrier for the Construction of a New Salicylate Membrane Sensor. Journal of the Chinese Chemical Society 54 (4):969-976. doi:10.1002/jccs.200700139

33. Yousry MI HI, Ola RS (2012). Journal of Electroanalytical Chemistry 666:11-18

34. Vamvakaki M, Chaniotakis NA (1996) Solid-contact ion-selective electrode with stable internal electrode. Analytica Chimica Acta 320 (1):53-61. doi:http://dx.doi.org/10.1016/0003-2670(95)00524-2

35. Szűcs J, Lindfors T, Bobacka J, Gyurcsányi RE (2016) Ion-selective Electrodes with 3D Nanostructured Conducting Polymer Solid Contact. Electroanalysis 28 (4):778-786. doi:10.1002/elan.201500465

36. Růžička J, Rald K (1971) The liquid-state, iodide-selective electrode. Analytica Chimica Acta 53 (1):1-12. doi:http://dx.doi.org/10.1016/S0003-2670(01)80064-7

37. Michalska A (2012) All-Solid-State Ion Selective and All-Solid-State Reference Electrodes. Electroanalysis 24 (6):1253-1265. doi:10.1002/elan.201200059

38. Kakhki S, Shams E, Barsan MM (2013) Fabrication of carbon paste electrode containing a new inorganic–organic hybrid based on [SiW12O40]4− polyoxoanion and Nile blue and its electrocatalytic activity toward nitrite reduction. Journal of Electroanalytical Chemistry 704:80-85. doi:http://dx.doi.org/10.1016/j.jelechem.2013.06.017

39. Ivanova NM, Levin MB, Mikhelson KN (2012) Problems and prospects of solid contact ion-selective electrodes with ionophore-based membranes. Russian Chemical Bulletin 61 (5):926-936. doi:10.1007/s11172-012-0136-0

40. Hu J, Stein A, Bühlmann P (2016) Rational design of all-solid-state ion-selective electrodes and reference electrodes. TrAC Trends in Analytical Chemistry 76:102-114. doi:http://dx.doi.org/10.1016/j.trac.2015.11.004

41. Brinić S, Buzuk M, Bralić M, Generalić E (2012) Solid-contact Cu(II) ion-selective electrode based on 1,2-di-(o-salicylaldiminophenylthio)ethane. Journal of Solid State Electrochemistry 16 (4):1333-1341. doi:10.1007/s10008-011-1528-z

42. Fierke MA, Lai C-Z, Bühlmann P, Stein A (2010) Effects of Architecture and Surface Chemistry of Three-Dimensionally Ordered Macroporous Carbon Solid Contacts on Performance of Ion-Selective Electrodes. Analytical Chemistry 82 (2):680-688. doi:10.1021/ac902222n

43. Ivanova NM, Podeshvo IV, Goikhman MY, Yakimanskii AV, Mikhelson KN (2013) Potassium-selective solid contact electrodes with poly(amidoacid) Cu(I) complex, electron-ion exchanging resin and different sorts of carbon black in the transducer layer. Sensors and Actuators B: Chemical 186:589-596. doi:http://dx.doi.org/10.1016/j.snb.2013.06.072

44. Paczosa-Bator B (2012) All-solid-state selective electrodes using carbon black. Talanta 93:424-427. doi:http://dx.doi.org/10.1016/j.talanta.2012.02.013

45. Saravia LPH, Anandhakumar S, Parussulo ALA, Matias TA, Caldeira da Silva CC, Kowaltowski AJ, Araki K, Bertotti M (2016) Development of a tetraphenylporphyrin cobalt (II) modified glassy carbon electrode to monitor oxygen consumption in biological samples. Journal of Electroanalytical Chemistry 775:72-76. doi:http://dx.doi.org/10.1016/j.jelechem.2016.05.026

46. Jarvis JM, Guzinski M, Pendley BD, Lindner E (2016) Poly(3-octylthiophene) as solid contact for ion-selective electrodes: contradictions and possibilities. Journal of Solid State Electrochemistry 20 (11):3033-3041. doi:10.1007/s10008-016-3340-2

47. Mikhelson K (2013) Ion-selective Electrodes, vol 81. Lecture Notes in Chemistry. Springer, Heidelberg-New York-Dordrecht-London

48. Bobacka J, Ivaska A, Lewenstam A (2008) Potentiometric Ion Sensors. Chemical Reviews 108 (2):329-351. doi:10.1021/cr068100w

49. Khripoun GA, Volkova EA, Liseenkov AV, Mikhelson KN (2006) Nitrate-Selective Solid Contact Electrodes with Poly(3-octylthiophene) and Poly(aniline) as Ion-to-Electron Transducers Buffered with Electron-Ion-Exchanging Resin. Electroanalysis 18 (13-14):1322-1328. doi:10.1002/elan.200603532

50. Dean J (1974) Lange's Handbook of chemistry. 15 edn.,

51. Kulapin AI, Chernova RK, Kulapina EG (2005) Some regularities of interface formation in solid-contact potentiometric surfactant-selective sensors. In English. Journal of Analytical Chemistry 60 (3):282-288. doi:10.1007/s10809-005-0085-y

52. Kulapin AI, Mikhailova AM, Kulapina EG (2003) Stabilizing Potential of Solid-Contact Sensors Selective towards Surface-Active Substances. In English. Russian Journal of Electrochemistry 39 (5):585-590. doi:10.1023/A:1023897431397

53. Kulapin AI, Chernova RK, Kulapina EG (2002) New Modified Electrodes for the Separate Determination of Polyoxyethylated Nonylphenols. In English. Journal of Analytical Chemistry 57 (7):638-643. doi:10.1023/A:1016242420872

54. Rezaei B, Meghdadi S, Nafisi V (2007) Fast response and selective perchlorate polymeric membrane electrode based on bis(dibenzoylmethanato) nickel(II) complex as a neutral carrier. Sensors and Actuators B: Chemical 121 (2):600-605. doi:http://dx.doi.org/10.1016/j.snb.2006.04.093

55. Valiotti AB, Vasil'eva OE, Starikova TA, Semeikin AS, Shumilova GI (2011) Electrochemical properties and spectrophotometry of membranes based on holmium tetraphenylporphyrinchloride. In English. Russian Journal of General Chemistry 81 (4):762. doi:10.1134/S1070363211040256

56. Moreno-Castilla C (2004) Adsorption of organic molecules from aqueous solutions on carbon materials. Carbon 42 (1):83-94. doi:http://dx.doi.org/10.1016/j.carbon.2003.09.022

57. Wang J, Wang F, Yao J, Guo H, Blake RE, Choi MMF, Song C (2013) Effect of pH and Temperature on Adsorption of Dimethyl Phthalate on Carbon Nanotubes in Aqueous Phase. Analytical Letters 46 (2):379-393. doi:10.1080/00032719.2012.713067

58. Starikova TA SG, Pendin AA (2012). Russian Journal of General Chemistry 82 (11):1909-1914

59. Chaniotakis N, Chasser A, Meyerhoff M, Groves J (1988) Influence of porphyrin structure on anion selectivities of manganese (III) porphyrin based membrane electrodes. Analytical chemistry 60 (2):185-188

60. Malinski T (2000) Porphyrin-based Electrochemical Sensors. In: Kadish KM, Smith KM, Guilard M (eds) The porphyrin handbook., vol 6. Academic Press., USA, pp 232-256.

61. Chou J-H, Kosal ME, Nalwa HS, Rakow NA, Suslick KS (2000) Applications of porphyrins and metalloporphyrins to materials chemistry. In: Kadish K, Smith KM, Guilard R (eds) The porphyrin handbook., vol 6. Academic Press, USA, pp 44-131

62. Zhai J, Xie X, Bakker E (2015) Ion-Selective Optode Nanospheres as Heterogeneous Indicator Reagents in Complexometric Titrations. Analytical Chemistry 87 (5):2827-2831. doi:10.1021/ac504213q

63. Hill CL, Williamson MM (1985) Structural and electronic properties of six-coordinate manganese (III) porphyrin cations. Crystal and molecular structure of bis (N, N-dimethylformamide)(tetraphenylporphinato) manganese (III) perchlorate,[MnIII TPP (DMF) 2]+ ClO4. Inorganic Chemistry 24 (18):2836-2841

64. Boucher LJ (1972) Manganese porphyrin complexes. Coordination Chemistry Reviews 7 (3):289-329. doi:http://dx.doi.org/10.1016/S0010-8545(00)80024-7

65. Boucher LJ (1968) Manganese porphyrin complexes. I. Synthesis and spectroscopy of manganese(III) protoporphyrin IX dimethyl ester halides. Journal of the American Chemical Society 90 (24):6640-6645. doi:10.1021/ja01026a014

66. Great Medical Encyclopedia (1981), vol 15. M. Soviet Encyclopedia,

67. Burns DT, Danzer K, Townshend A (2002) Use of the Term "Recovery" and "Apparent Recovery" in Analytical Procedures (IUPAC Recommendations 2002). Pure Appl Chem 74:2201-2205

68. Koch-Weser J (1972) Serum Drug Concentrations as Therapeutic Guides. N Engl J Med 287:227-231

69. Pau CP, Rechnitz GA (1984) Bound coefactor/dual enzyme electrode system for l-alanine. Analytica Chimica Acta 160:141-147. doi:http://dx.doi.org/10.1016/S0003-2670(00)84515-8

70. Ganjali MR, Kiani-Anbouhi R, Pourjavid MR, Salavati-Niasari M (2003) Bis (trans-cinnamaldehyde) ethylene diimine dibromonickel (II) complex as a neutral carrier for salicylate-selective liquid membrane and coated graphite sensors. Talanta 61 (3):277-284. doi:http://dx.doi.org/10.1016/S0039-9140(03)00273-X

71. Chernyshov DV, Egorov VM, Shvedene NV, Pletnev IV (2009) Low-Melting Ionic Solids: Versatile Materials for Ion-Sensing Devices. ACS Applied Materials & Interfaces 1 (9):2055-2059. doi:10.1021/am9004072